Reactions of Laser-Ablated Cu with NO: Infrared Spectra and Density Functional Calculations of $CuNO^+$, CuNO, $Cu(NO)_2$, and $Cu(NO)_2^-$ in Solid Neon and Argon

Mingfei Zhou[†] and Lester Andrews*

Department of Chemistry, University of Virginia, Charlottesville, Virginia 22904-4319

Received: October 1, 1999; In Final Form: December 13, 1999

Laser-ablated copper atoms react with NO molecules in excess neon and argon during condensation to form the CuNO and $Cu(NO)_2$ complexes as major products and $Cu(NO)_2(NO)$* as a minor product. In addition, the $CuNO^+$ cation and $Cu(NO)_2^-$ anion are also formed. The product absorptions are identified from isotopic shifts and splitting patterns in the matrix infrared spectra and are supported by DFT calculations of isotopic frequencies. Sequential annealing increases CuNO and $Cu(NO)_2$, and then CuNO gives way to $Cu(NO)_2$ and $Cu(NO)_2(NO)$*, a dinitrosyl with a third inequivalent NO subgroup. The isolated mononitrosyl and dinitrosyl species provide a scale to estimate local charge on CuNO and $Cu(NO)_2$ sites in Cu-exchanged zeolite catalyst systems.

Introduction

The reactions of nitric oxide with transition metals are of interest as nitric oxides are the main pollutants in the fuel combustion process, and their removal involves catalytic reduction on the metal surface. Copper-exchanged zeolites have high activities in the catalytic reduction of NO,[1,2] and considerable experimental and theoretical work has been done to understand the reduction mechanisms.[1−10] In particular, Cu−*gem*-dinitrosyl species have been suggested to play an important role in N−N bond formation and decomposition to N_2 and O_2.[2,5−7] The interaction of NO with bare metal atoms and cations has also been studied. Schwarz and co-workers have investigated CuNO and $CuNO^+$ with collisional activation mass spectrometry and suggested that the molecules have either a side-on geometry or two rapidly interconverting end-on geometries.[11] The reaction of thermally generated copper atoms with NO has been examined in an argon matrix, which reported copper mononitrosyl and dinitrosyl complexes.[12]

Computational studies of CuNO, $CuNO^+$, and their isomers have been conducted by Hrusak et al. with CCSD(T) and by Benjelloun et al. with self-consistent field (SCF) and configuration interaction (CI) methods.[13,14] The CuNO and $CuNO^+$ species have been reinvestigated in more recent theoretical studies using DFT methods.[15,16] Finally, the chemisorption of nitric oxide on the copper metal surface has been thoroughly investigated using a variety of experimental techniques,[17,18] and the bonding of NO to copper clusters has also been studied.[19,20]

Laser ablation is an effective method for producing clean metal atoms, cations, and electrons for matrix isolation study. By co-deposition of laser-ablated transition metal atoms, cations, and electrons with CO, metal carbonyl cations and anions as well as neutral molecules have been formed.[21−23] These isolated carbonyl species provide a scale to estimate charge on metal carbonyl complexes in rhodium carbonyl catalyst systems.[23] In this paper, we report the reactions of laser-ablated copper with NO in excess argon and neon. We will show that previous assignments[12] to copper mono- and dinitrosyl complexes *must be reversed* on the basis of *new mixed isotopic spectra* and DFT isotopic frequency calculations. In addition, the copper mononitrosyl cation and dinitrosyl anion will also be identified.

Experimental Section

The experiment for laser ablation and matrix isolation spectroscopy has been described in detail previously.[24] Briefly, the Nd:YAG laser fundamental (1064 nm, 10 Hz repetition rate with 10 ns pulse width) was focused on the rotating copper metal target (Johnson Matthey, 99.9998%) using low energy (1−5 mJ/pulse). Laser-ablated copper atoms, cations, and electrons were co-deposited with nitric oxide (0.1−0.5%) in excess neon and argon onto a 4 or 10 K CsI cryogenic window at 2−4 mmol/h for 30 min to 2 h, giving approximate copper atom concentrations of 0.01% in neon and 0.1% in argon samples. Nitric oxide (Matheson), isotopic $^{15}N^{16}O$ and $^{15}N^{18}O$ (Isomet, 99%) and selected mixtures were used in different experiments. Infrared spectra were recorded at 0.5 cm^{-1} resolution on a Nicolet 750 spectrometer with 0.1 cm^{-1} accuracy using a HgCdTe detector. Matrix samples were annealed at different temperatures, and selected samples were subjected to broad-band photolysis by a medium-pressure mercury arc (Philips, 175W) with the globe removed and glass filters.

Results

Infrared spectra in the 1710−1490 cm^{-1} region from co-deposition of laser-ablated copper with NO in excess neon on a 4 K substrate are shown in Figure 1, and the product absorptions are listed in Table 1. Metal-independent absorptions, which are common to other NO reaction systems, have been reported previously and are not listed here.[25,26] Different temperature annealing and photolysis were conducted as shown in Figure 1. Experiments were done using $^{15}N^{16}O$ and $^{15}N^{18}O$ samples, and very similar spectra were obtained. The isotopic frequencies are listed in Table 1. Similar experiments with $^{14}N^{16}O + {}^{15}N^{16}O$ and $^{15}N^{16}O + {}^{15}N^{18}O$ mixtures were also performed, and diagnostic spectra in different regions are shown in Figures 2−4. Experiments were done with CCl_4 added (10% of NO) to serve as an electron trap.[21−23]

* To whom correspondence should be addressed. E-mail: lsa@virginia.edu.
[†] Permanent address: Laser Chemistry Institute, Fudan University, Shanghai, People's Republic of China.

10.1021/jp993516h CCC: $19.00
Published on Web 03/08/2000

TABLE 1: Infrared Absorptions (cm^{-1}) from Co-deposition of Laser-Ablated Copper Atoms with Nitric Oxides in Excess Neon

$^{14}N^{16}O$	$^{15}N^{16}O$	$^{15}N^{18}O$	$^{14}N^{16}O + {}^{15}N^{16}O$	$^{15}N^{16}O + {}^{15}N^{18}O$	*R*(14/15)	*R*(16/18)	assignment
3412.5	3345.9	3271.4	3412.5, 3380.5, 3345.9	3345.9, 3310.3, 3271.4	1.0199	1.0228	$Cu(NO)_2$ site
3407.6	3341.1	3266.8	3407.6, 3375.6, 3341.1	3341.2, 3305.5, 3266.8	1.0199	1.0227	$Cu(NO)_2$ site
3406.0	3339.4	3265.3	3406.0, 3373.9, 3339.4	3339.5, 3303.9, 3265.3	1.0199	1.0227	$Cu(NO)_2$
3401.0	3334.7	3260.4	3401.0, 3369.0, 3334.7	3334.7, 3298.9, 3260.4	1.0199	1.0228	$Cu(NO)_2$
1907.9							$CuNO^+$
1692.8	1662.8	1618.9	1692.8, 1687.7, 1680.3, 1676.4, 1665.8, 1662.9	1662.8, 1654.9, 1645.0, 1639.4, 1622.6, 1619.1	1.0180	1.0271	$Cu(NO)_2(NO)^*$
1642.0	1609.4	1574.6	1642.0, 1623.8, 1609.4	1609.4, 1589.6, 1574.6	1.0203	1.0221	$Cu(NO)_2$ site
1638.7	1606.2	1571.6	1638.7, 1620.6, 1606.2	1606.2, 1586.6, 1571.6	1.0202	1.0220	$Cu(NO)_2$ site
1637.2	1604.7	1570.2	1637.2, 1619.2, 1604.7	1604.7, 1585.2, 1570.2	1.0203	1.0220	$Cu(NO)_2$
1635.5	1603.0	1658.5	1635.5, 1617.4, 1603.0	1603.1, 1583.6, 1568.5	1.0203	1.0220	$Cu(NO)_2$
1602.2	1574.6	1532.0	1602.2, 1574.6	1574.6, 1532.0	1.0175	1.0278	CuNO
1565.2	1533.2	1500.8	1565.1, 1544.3, 1533.2	1533.2, 1511.3, 1500.8	1.0209	1.0216	$Cu(NO)_2^-$
1561.3	1529.4	1497.0	1561.4, 1540.6, 1529.4	1529.4, 1507.2, 1497.1	1.0209	1.0216	$Cu(NO)_2^-$ site
1499.6	1473.7	1433.8	1499.7, 1485.7, 1473.7	1473.7, 1451.5, 1433.8	1.0176	1.0278	$Cu_2(NO)_2$
1214.5	1191.4	1163.4	1214.4, 1191.5	1191.0, 1174.9, 1163.3	1.0194	1.0241	Cu[OO]N
615.1	609.4	599.1			1.0094	1.0172	$^{63}Cu(NO)_2$
611.1	605.4				1.0094		$^{65}Cu(NO)_2$

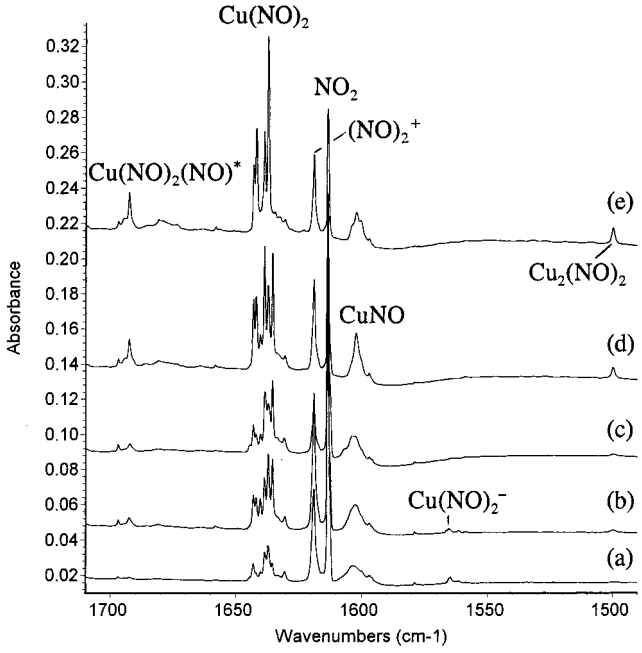

Figure 1. Infrared spectra in the 1710−1490 cm^{-1} region for laser-ablated copper atoms co-deposited with 0.1% NO in neon: (a) after 30 min of sample deposition at 4 K, (b) after annealing to 8 K, (c) after 15 min of full arc photolysis, (d) after annealing to 10 K, and (e) after annealing to 12 K.

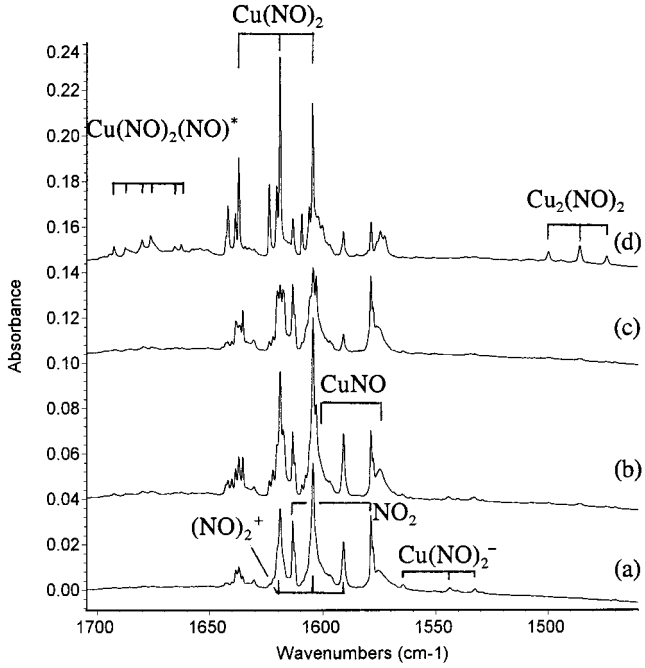

Figure 2. Infrared spectra in the 1705−1460 cm^{-1} region for laser-ablated copper atoms co-deposited with 0.05% $^{14}N^{16}O$ + 0.05% $^{15}N^{16}O$ in neon: (a) after 45 min of sample deposition at 4 K, (b) after annealing to 8 K, (c) after 15 min of full arc photolysis, and (d) after annealing to 12 K.

Complementary experiments were also done in an argon matrix on a 10 K cryogenic window using 4 times the laser energy employed for the neon experiments. Figure 5 shows the spectra in the 1880−1500 cm^{-1} region with 0.3% NO in argon, and the absorptions are listed in Table 2. Similar experiments were done with $^{15}N^{16}O$ and $^{14}N^{16}O + {}^{15}N^{16}O$ samples, and Figure 6 shows the spectra in the 1880−1490 cm^{-1} region with a 0.3% $^{14}N^{16}O + {}^{15}N^{16}O$ sample.

Density functional calculations (DFT) were employed for band identifications using the Gaussian 94 program.[27] The BP86 and hybrid B3LYP functionals in conjunction with the 6-311+G-(d) basis set on N and O atoms and the all-electron set of Wachters and Hay for Cu atom as provided by Gaussian 94 were used.[28−31] The geometries were fully optimized and the harmonic vibrational frequencies computed using second derivatives. Calculations were first performed on $CuNO^+$, CuNO, and $CuNO^-$ using both functionals, and the results are listed in Tables 3 and 4. Similar calculations were also done on $Cu(NO)_2$ neutral, cation, and anion with both functionals, and the results are listed in Table 5. Analogous calculations performed for the $Cu(NO)_2(NO)^*$ species are summarized in Table 6 and Figure 7. Finally, similar calculations were done for dicopper nitrosyls as summarized in Table 7.

Discussion

Copper nitrosyl cations, neutrals, and anions will be identified from isotopic substitution, isotopic mixtures, and DFT isotopic frequency calculations.

CuNO. The strong band observed at 1602.2 cm^{-1} in neon experiments after sample deposition slightly increased and sharpened on 8 and 10 K annealing, and then decreased on 12 K annealing while the 1637.2 cm^{-1} band increased. The 1602.2 cm^{-1} band shifted to 1574.6 cm^{-1} with $^{15}N^{16}O$ and to 1532.0 cm^{-1} with the $^{15}N^{18}O$ sample, and gave a $^{14}NO/^{15}NO$ ratio of 1.0175 and a $^{15}N^{16}O/^{15}N^{18}O$ ratio of 1.0278. In the mixed $^{14}N^{16}O + {}^{15}N^{16}O$ and $^{15}N^{16}O + {}^{15}N^{18}O$ experiments, *only pure isotopic*

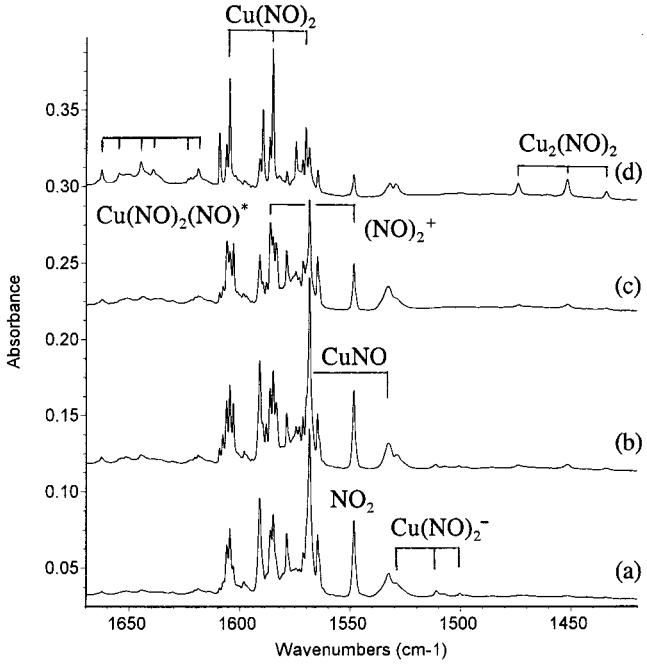

Figure 3. Infrared spectra in the 1670−1420 cm^{-1} region for laser-ablated copper atoms co-deposited with 0.05% $^{15}N^{16}O$ + 0.05% $^{15}N^{18}O$ in neon: (a) after 45 min of sample deposition at 4 K, (b) after annealing to 8 K, (c) after 15 min of full arc photolysis, and (d) after annealing to 12 K.

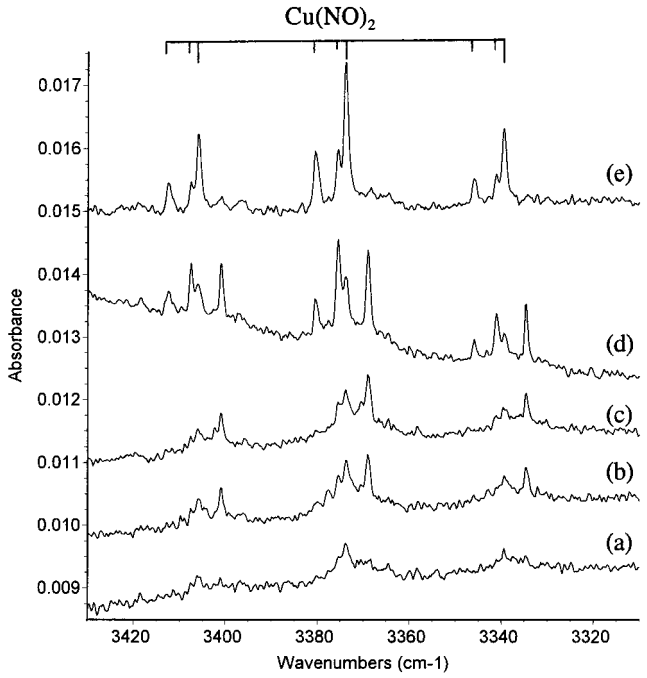

Figure 4. Infrared spectra in the 3430−3310 cm^{-1} region for laser-ablated copper atoms co-deposited with 0.05% $^{14}N^{16}O$ + 0.05% $^{15}N^{16}O$ in neon: (a) after 45 min of sample deposition at 4 K, (b) after annealing to 8 K, (c) after 15 min of full arc photolysis, (d) after annealing to 10 K, and (e) after annealing to 12 K.

counterparts were observed, indicating that only one NO subunit is involved in this mode. This band is assigned to the N−O stretching vibration of the CuNO molecule. The corresponding CuNO absorption was observed here at 1587.1 cm^{-1} in argon, red-shifted 15.1 cm^{-1} from the neon matrix band position, and showed a doublet in our mixed $^{14}N^{16}O$ + $^{15}N^{16}O$ experiment. Chiarelli and Ball previously assigned argon matrix 1610.5 and 608.8 cm^{-1} bands to N−O and Cu−N stretching vibrations of

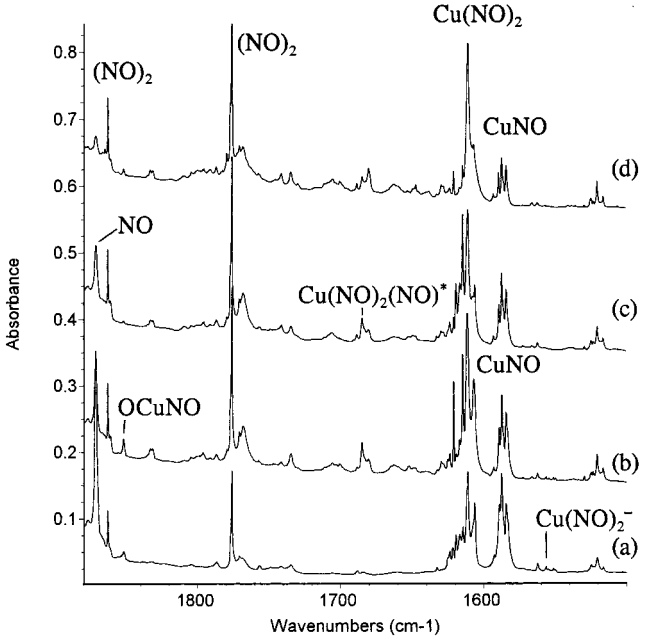

Figure 5. Infrared spectra in the 1880−1500 cm^{-1} region for laser-ablated copper atoms co-deposited with 0.3% NO in argon: (a) after 60 min of sample deposition at 10 K, (b) after annealing to 25 K, (c) after 15 min of full arc photolysis, and (d) after annealing to 35 K.

TABLE 2: Infrared Absorptions (cm^{-1}) from Co-deposition of Laser-Ablated Copper Atoms with Nitric Oxides in Excess Argon

$^{14}N^{16}O$	$^{15}N^{16}O$	$^{14}N^{16}O$ + $^{15}N^{16}O$	*R*(14/15)	assignment
3380.8	3314.9	3380.8, 3348.9, 3315.0	1.0199	$Cu(NO)_2$ site
3373.2	3307.5	3373.1, 3341.4, 3307.5	1.0199	$Cu(NO)_2$
3364.8	3299.2	3365.0, 3332.8, 3299.6	1.0199	$Cu(NO)_2$ site
1852.2	1816.2	1852.2, 1816.2	1.0198	OCuNO
1734.8	1702.7	1734.6, 1702.6	1.0189	(CuCuNO)
1684.9	1654.8		1.0182	$Cu(NO)_2(NO)$*
1680.0	1650.1		1.0181	$Cu(NO)_2(NO)$*
1614.7	1582.7	1614.7, 1597.1, 1582.7	1.0202	$Cu(NO)_2$ site
1611.6	1579.6	1611.8, 1594.2, 1579.8	1.0203	$Cu(NO)_2$
1606.9	1575.1	1606.9, 1589.2, 1575.1	1.0202	$Cu(NO)_2$ site
1587.1	1559.0	1587.4, 1559.1	1.0180	CuNO
1556.6	1524.6		1.0210	$Cu(NO)_2^-$
1551.2	1519.4		1.0209	$Cu(NO)_2^-$
1549.9	1518.0		1.0210	$Cu(NO)_2^-$ site
1529.3	1500.4	1529.3, 1500.4	1.0193	Cu_2NO site
1524.5	1495.7	1524.5, 1495.7	1.0193	Cu_2NO site
1520.4	1492.6	1520.4, 1492.6	1.0186	?
1515.9	1488.3	1515.9, 1488.3	1.0185	?
1213.4	1190.8	1213.4, 1190.8	1.0190	Cu[OO]N
608.6	603.6	608.6, 606.1, 603.6	1.0083	$^{63}Cu(NO)_2$
604.8	599.6		1.0087	$^{65}Cu(NO)_2$

the CuNO molecule according to different NO concentration experiments.[12] As will be discussed below, the 1610.5 cm^{-1} band (corresponding to 1611.6 cm^{-1} in our argon matrix absorption) clearly exhibited a triplet isotopic structure with approximately 1:2:1 relative intensities in our mixed $^{14}N^{16}O$ + $^{15}N^{16}O$ experiment, which indicates a dinitrosyl species. The 1586.0 cm^{-1} band, which Chiarelli and Ball assigned to the $Cu(NO)_2$ molecule, must now be reassigned to the CuNO molecule. In contrast to Chiarelli and Ball, we find that annealing solid argon from 12 to 25 K (Figure 5a,b) decreases our CuNO band (1587.2 cm^{-1}), increases our $Cu(NO)_2$ band (1611.6 cm^{-1}), and markedly increases a very weak 1684.9 cm^{-1} absorption, which will be assigned below to $Cu(NO)_2(NO)$* on the basis of the *sextet pattern* in the mixed isotopic spectrum (neon matrix spectrum (Figure 3)). Clearly, on diffusion CuNO

TABLE 3: Calculated Geometries, Relative Energies (kcal/mol), Mulliken Charges, and Dipole Moments (D) for CuNO, CuON, $CuNO^+$, $CuON^+$, and $CuNO^-$

	molecule	energy	geometry	Cu	N	O	D
B3LYP	CuNO (^{1}A′)	0	Cu−N 1.944 Å, N−O 1.174 Å, ∠CuNO 119.1°	−0.02	−0.04	+0.06	1.6
	CuNO (^{3}A″)	−3.1	Cu−N 1.885 Å, N−O 1.194 Å, ∠CuNO 129.9°	+0.12	−0.09	−0.03	3.2
	CuON (^{3}A″)	+9.9	Cu−O 1.990 Å, N−O 1.206 Å, ∠CuON 128.6°	+0.18	−0.18	0.00	2.7
	$CuNO^+$ (^{2}A′)	+171.6	Cu−N 1.962 Å, N−O 1.133 Å, ∠CuNO 133.6°	+0.63	+0.12	+0.25	1.8
	$CuON^+$ (^{2}A′)	+181.7	Cu−O 2.078 Å, N−O 1.152 Å, ∠CuON 134.9°	+0.77	+0.07	+0.16	1.8
	$CuNO^-$ (^{2}A″)	−35.9	Cu−N 1.959 Å, N−O 1.232 Å, ∠CuNO 122.9°	−0.52	−0.28	−0.19	0.3
BP86	CuNO (^{1}A′)	0	Cu−N 1.901 Å, N−O 1.185 Å, ∠CuNO 120.3°	−0.11	+0.03	+0.08	0.8
	CuNO (^{3}A″)	+2.9	Cu−N 1.837 Å, N−O 1.204 Å, ∠CuNO 132.0°	+0.02	−0.02	0.00	2.4
	CuON (^{3}A″)	+19.0	Cu−O 1.947 Å, N−O 1.218 Å, ∠CuON 129.6°	+0.13	−0.20	+0.07	2.3
	$CuNO^+$ (^{2}A′)	+181.8	Cu−N 1.889 Å, N−O 1.146 Å, ∠CuNO 132.6°	+0.54	+0.18	+0.28	1.5
	$CuON^+$ (^{2}A′)	+197.2	Cu−O 2.030 Å, N−O 1.159 Å, ∠CuON 133.7°	+0.67	+0.07	+0.26	1.2
	$CuNO^-$ (^{2}A″)	−34.2	Cu−N 1.910 Å, N−O 1.241 Å, ∠CuNO 121.6°	−0.64	−0.20	−0.16	0.5

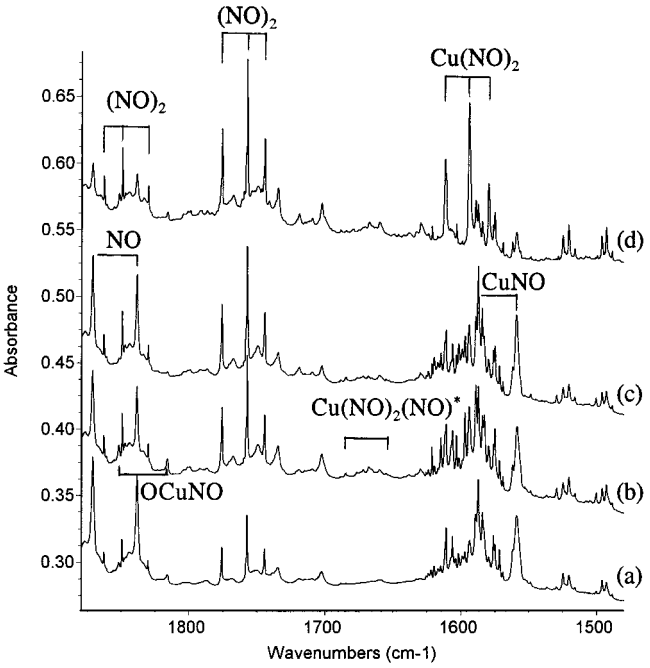

Figure 6. Infrared spectra in the 1880−1490 cm^{-1} region for laser-ablated copper atoms co-deposited with 0.15% $^{14}N^{16}O$ + 0.15% $^{15}N^{16}O$ in argon: (a) after 60 min of sample deposition at 10 K, (b) after annealing to 25 K, (c) after 15 min of full arc photolysis, and (d) after annealing to 35 K.

TABLE 4: Calculated Vibrational Freqencies (cm^{-1}) and Intensities (km/mol) (in Parentheses) for the Structures Described in Table 3

	molecule	N−O stretch	M−N stretch	MNO bend
B3LYP	CuNO (^{1}A′)	1703.3 (1180)	470.9 (18)	281.3 (3)
		1673.3[a]	457.8	279.6
		1626.8[b]	455.2	270.8
	CuNO (^{3}A″)	1618.3 (1344)	412.1 (5)	223.8 (7)
	CuON (^{3}A″)	1400.4 (1806)	304.4 (26)	178.4 (18)
	$CuNO^+$ (^{2}A′)	2001.5 (297)	328.8 (6)	218.1 (2)
	$CuON^+$ (^{2}A′)	1849.2 (181)	256.1 (1)	183.0 (1)
	$CuNO^-$ (^{2}A″)	1454.8 (1023)	376.2 (16)	218.8 (2)
BP86	CuNO (^{1}A′)	1650.2 (875)	486.6 (15)	292.1 (3)
	CuNO (^{3}A″)	1596.2 (761)	450.9 (6)	232.5 (6)
	CuON (^{3}A″)	1430.1 (665)	329.5 (4)	195.2 (2)
	$CuNO^+$ (^{2}A′)	1878.8 (472)	384.1 (11)	247.6 (2)
	$CuON^+$ (^{2}A′)	1730.5 (390)	286.6 (7)	199.4 (3)
	$CuNO^-$ (^{2}A″)	1399.7 (1015)	426.8 (22)	248.9 (3)

[a] Frequencies for $^{15}N^{16}O$. [b] Frequencies for $^{15}N^{18}O$.

reacts with more NO to form higher complexes, and $(NO)_2$ increases likewise at the expense of NO on annealing.

CuNO has been the subject of several theoretical studies. Schwarz and co-workers found that a ^{3}A″ state is more stable than the ^{1}A′ state at the SCF, CISD, and CCSD levels of theory, while the CCSD(T) method convincingly shows that the ^{1}A′ state is the ground state.[13] Salahub and co-workers also predicted a ^{1}A′ ground state for CuNO using the DFT/BPW method.[16] As listed in Table 3, our DFT calculations found the ^{1}A′ state 2.9 kcal/mol lower in energy than the ^{3}A″ state using BP86, but the ^{3}A″ state 3.1 kcal/mol lower in energy using the B3LYP functional. As has been discussed in detail,[16] both the ^{1}A′ and ^{3}A″ states have bent structures. The ^{3}A″ state CuNO was predicted to have shorter Cu−N and longer N−O bond lengths and, hence, a lower N−O stretching vibrational frequency. The calculated frequencies and isotopic ratios are essentially the same for both states, which makes it difficult to determine which state is the ground state. However, the calculated (B3LYP) isotopic frequency ratios for $^{14}N^{16}O/^{15}N^{16}O$ (1.0179) and $^{15}N^{16}O/^{15}N^{18}O$ (1.0286) are in excellent agreement with the observed ratios (1.0175 and 1.0278). These ratios are similar to the isotopic frequency ratios observed for NO itself (1.0179 and 1.0277) and show little N−O interaction with the Cu−N vibrational mode in contrast to $Cu(NO)_2$ discussed below.

The Cu + NO reaction is exothermic by 10.4 kcal/mol at the CCSD(T) level of theory.[13]

$$Cu + NO \rightarrow CuNO\ (^1A'_1) \qquad (1)$$

This reaction proceeds on annealing in both solid argon and neon.

$Cu(NO)_2$. The bands centered at 1637.2 cm^{-1} in neon slightly decreased on photolysis, but markedly increased on annealing. The isotopic $^{14}NO/^{15}NO$ ratio of 1.0203 and $^{15}N^{16}O/^{15}N^{18}O$ ratio of 1.0220 are characteristic of nitrosyl N−O stretching vibrational frequency ratios where vibrational coupling has *increased* N and *decreased* O participation. In both mixed $^{14}N^{16}O$ + $^{15}N^{16}O$ and $^{15}N^{16}O$ + $^{15}N^{18}O$ isotopic experiments, triplets with approximately 1:2:1 relative intensities were produced, which confirms that *two equivalent NO submolecules* are involved in this vibrational mode; accordingly, these bands are assigned to the antisymmetric N−O stretching vibration of the $Cu(NO)_2$ molecule in different matrix sites. The absence of the symmetric vibrational absorption suggests that the $Cu(NO)_2$ molecule is linear. Weak bands centered at 3406.0 cm^{-1} have exactly the same site structure, annealing, and photolysis behavior, suggesting different vibrational modes of the same molecule. This band has about 3.2% of the intensity of the 1637.2 cm^{-1} band. The 3406.0 cm^{-1} band shifted to 3339.4 cm^{-1} with $^{15}N^{16}O$ and to 3265.3 cm^{-1} with the $^{15}N^{18}O$ sample, and gave a $^{14}NO/^{15}NO$ ratio of 1.0199 and a $^{15}N^{16}O/^{15}N^{18}O$ ratio of 1.0228, which are appropriate for N−O stretching vibrational ratios. This region is much too high for a N−O stretching fundamental, and it must be considered for a combination or overtone band. The difference for each isotopic molecule, 3406.0 − 1637.2 =

TABLE 5: Calculated Geometries, Relative Energies (kcal/mol), and Vibrational Frequencies (cm^{-1}) and Intensities (km/mol) (in Parentheses) for $Cu(NO)_2$, $Cu(NO)_2^+$, and $Cu(NO)_2^-$

	molecule	relative energy	geometry	sym N−O	asym N−O	asym M−N
B3LYP	$Cu(NO)_2$ ($^2\Pi_u$)	0	Cu−N 1.712 Å, N−O 1.171 Å	1884.5 (0)[a]	1798.8 (2547)	637.9 (19)
				1847.0 (0)[b]	1762.5 (2456)	634.1 (17)
				1803.0 (0)[c]	1721.8 (2324)	621.6 (19)
	$Cu(NO)_2$ ($^4\Pi_g$)	−15.6	Cu−N 1.791 Å, N−O 1.180 Å, linear	1854.7 (0)[a]	1702.3 (3933)	511.2 (19)
				1818.8 (0)[b]	1669.2 (3795)	507.7 (18)
				1773.7 (0)[c]	1628.3 (3587)	498.5 (19)
	$Cu(NO)_2$ ($^2B_1$)	+11.4	Cu−N 2.011 Å, N−O 1.164 Å, ∠NCuN 74.1°, ∠CuNO 127.8°	1809.3 (552)	1758.3 (1529)	531.2 (7)
	$Cu(NO)_2^+$ ($^3\Sigma_g^-$)	+170.2	Cu−N 1.779 Å, N−O 1.134 Å, linear	2069.0 (0)	1942.1 (3232)	529.6 (0.8)
	$Cu(NO)_2^+$ ($^1A_1$)	+183.2	Cu−N 2.108 Å, N−O 1.126 Å, ∠NCuN 75.1°, ∠CuNO 124.6°	2020.1 (340)	1924.6 (1999)	502.7 (6)
	$Cu(NO)_2^-$ ($^1\Sigma_g^+$)	−39.8	Cu−N 1.682 Å, N−O 1.212 Å, linear	1681.4 (0)	1625.2 (2697)	675.3 (112)
	$Cu(NO)_2^-$ ($^3B_2$)	−46.5	Cu−N 1.764 Å, N−O 1.225 Å, ∠NCuN 170.9°, ∠CuNO 152.0°	1601.4 (6)	1517.0 (2617)	583.7 (44)
BP86	$Cu(NO)_2$ ($^2\Pi_u$)	0	Cu−N 1.709 Å, N−O 1.186 Å, linear	1812.8 (0)[a]	1738.8 (1927)	626.7 (23)
				1776.0 (0)[b]	1703.4 (1857)	623.1 (21)
				1734.8 (0)[c]	1664.8 (1754)	610.6 (23)
	$Cu(NO)_2$ ($^4A_2$)	−0.3	Cu−N 1.806 Å, N−O 1.196 Å, ∠NCuN 168.9°, ∠CuNO 141.5°	1713.2 (0.7)[a]	1627.6 (1788)	522.6 (5)
				1681.1 (0.7)[b]	1597.2 (1726)	515.5 (4)
				1637.6 (0.6)[c]	1555.8 (1631)	510.2 (5)
	$Cu(NO)_2$ ($^2B_1$)	−15.0	Cu−N 1.950 Å, N−O 0.183 Å, ∠NCuN 83.9°, ∠CuNO 125.5°	1703.1 (335)	1618.9 (1850)	494.5 (0.4)
	$Cu(NO)_2^+$ ($^3\Sigma_g^-$)	+178.5	Cu−N 1.766 Å, N−O 1.149 Å	1981.6 (0)	1887.7 (1997)	531.6 (0.2)
	$Cu(NO)_2^+$ ($^1A_1$)	+195.2	Cu−N 2.036 Å, N−O 1.143 Å, ∠NCuN 82.4°, ∠CuNO 123.7°	1902.7 (256)	1841.2 (1365)	473.0 (6)
	$Cu(NO)_2^-$ ($^1\Sigma_g^+$)	−46.5	Cu−N 1.684 Å, N−O 1.228 Å	1623.2 (0)	1577.5 (2025)	661.6 (100)
	$Cu(NO)_2^-$ ($^3B_2$)	−37.1	Cu−N 1.759 Å, N−O 1.239 Å, ∠NCuN 168.1°, ∠CuNO 150.4°	1530.6 (0.8)	1472.4 (1751)	580.8 (44)

[a] $^{14}N^{16}O$ frequencies. [b] $^{15}N^{16}O$ frequencies. [c] $^{15}N^{18}O$ frequencies.

TABLE 6: Calculated (BP86/6-311+G(d)) Geometries and N−O Stretching Frequencies (cm^{-1}) and Intensities (km/mol) for the $Cu(NO)_2(NO)^*$ Complex

	geometry (bond lengths in angstroms, bond angles in degrees)	$^{14}N^{16}O$ freq int	$^{15}N^{16}O$	$^{15}N^{18}O$
$^3A''$	Cu−N 1.860, N−O 1.189, ∠Cu−N−O 168.0, ∠N−Cu−N 133.7,	1639.9 (2044) (a″)	1610.1	1567.0
	Cu−N* 1.919, N*−O 1.183, ∠Cu−N*−O 125.7, ∠N−Cu−N* 113.1	1640.4 (1089) (a′)	1611.0	1567.2
		1747.0 (17) (a′)	1715.2	1669.3
$^1A'$	Cu−N 1.727, N−O 1.185, ∠Cu−N−O 165.0, ∠N−Cu−N 162.4,	1701.4 (915) (a′)	1670.3	1625.8
	Cu−N* 2.137, N*−O 1.168, ∠Cu−N*−O 117.5, ∠N−Cu−N* 98.8	1726.0 (1960) (a″)	1691.7	1651.8
		1812.7 (24) (a′)	1777.8	1733.4

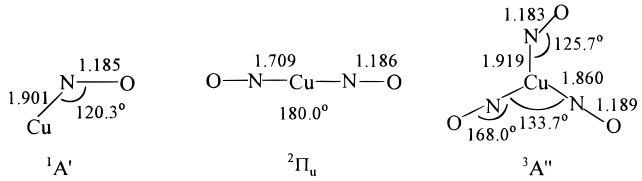

Figure 7. Structures of CuNO, $Cu(NO)_2$, and $Cu(NO)_2(NO)^*$ from BP86/6-311G(d) calculations (bond lengths in angstroms, angles in degrees).

1768.8 cm^{-1}, 3339.4 − 1604.7 = 1734.7 cm^{-1}, and 3265.3 − 1570.2 = 1695.1 cm^{-1}, gave a $^{14}NO/^{15}NO$ ratio of 1.0197 and a $^{15}N^{16}O/^{15}N^{18}O$ ratio of 1.0234, which are appropriate for a symmetric N−O stretching vibration (the B3LYP calculation predicts 1.0203 and 1.0244). The triplet isotopic structure in mixed $^{14}N^{16}O$ + $^{15}N^{16}O$ and $^{15}N^{16}O$ + $^{15}N^{18}O$ experiments (Figure 3) further confirms the $Cu(NO)_2$ assignment as does the combination band involving *two different* N−O stretching fundamentals. This band is assigned to the combination band of symmetric and antisymmetric N−O stretching vibrations of the linear $Cu(NO)_2$ molecule. Very weak bands at 615.1 and 611.1 cm^{-1} track with the 1637.2 and 3406.0 cm^{-1} bands and exhibit the intensity distribution for natural abundance copper isotopes. This 615.1 cm^{-1} doublet clearly indicates the involvement of one copper atom. These two bands are assigned to the antisymmetric ON−Cu−NO stretching vibration of the $^{63}Cu(NO)_2$ and $^{65}Cu(NO)_2$ isotopic molecules.

In our argon matrix, the antisymmetric N−O stretching vibration of the $Cu(NO)_2$ molecule is observed at 1611.6 cm^{-1}, which exhibited the same 14/15 isotopic ratio as the neon matrix band. The combination band is observed at 3373.2 cm^{-1} in argon, which gave a 1761.6 cm^{-1} symmetric N−O stretching vibrational frequency. The antisymmetric ON−Cu−NO vibrational modes of $^{63}Cu(NO)_2$ and $^{65}Cu(NO)_2$ are observed at 608.6 and 604.8 cm^{-1}, which shifted to 603.6 and 599.6 cm^{-1} in the $^{15}N^{16}O$ spectrum. The triplet mixed isotopic structure and the combination band of symmetric and antisymmetric N−O stretching vibrations confirm the dinitrosyl assignment and indicate that the previous assignment[12] is incorrect.

DFT calculations were performed to support the $Cu(NO)_2$ assignment. At the BP86/6-311+G* level of theory, linear $^2\Pi_u$ and bent $^4A_2$ states are found to be nearly identical in energy, and a bent $^2B_1$ state is about 15.3 kcal/mol higher in energy. The $^2\Pi_u$ state exhibited shorter Cu−N and N−O bond lengths than the $^4A_2$ state, and gave higher N−O and Cu−NO stretching vibrational frequencies as listed in Table 5. At the B3LYP/6-311+G* level of theory, a linear quartet state is predicted to be the most stable, with the linear $^2\Pi_u$ and the bent $^2B_1$ states lying 15.6 and 27.0 kcal/mol higher in energy. The calculated frequencies for the $^2\Pi_u$ state fit the experimental values much better, and both functionals predicted the symmetric N−O stretching and antisymmetric Cu−NO stretching vibrational frequencies of the quartet state too low. This comparison strongly suggests a $^2\Pi_u$ ground state for the $Cu(NO)_2$ molecule. Finally, calculations predict the antisymmetric ON−Cu−NO stretching near 600 cm^{-1} for the $Cu(NO)_2$ molecule and further confirm the present reassignment since the Cu−NO vibration is predicted below 500 cm^{-1}. In addition, both functionals predict isotopic frequency ratios ($^{14}N^{16}O/^{15}N^{16}O$, 1.0208, 1.0206; $^{15}N^{16}O/^{15}N^{18}O$, 1.0232, 1.0236) that effectively model the

TABLE 7: Calculated (BP86/6-311+G*) Geometries and N−O Stretching Vibrational Frequencies (cm^{-1}) and Intensities (km/mol) for the OCuNO, Cu_2NO and $Cu_2(NO)_2$ Molecules

molecule	geometry (bond lengths in angstroms, bond angles in degrees)	freq (int)
OCuNO ($^1\Sigma^+$)	O−Cu 1.660, Cu−N 1.687, N−O 1.162, angles 180	1890.0 (775) 870.7 (26), 522.8 (1)
CuCuNO ($^2A'$)	Cu−Cu 2.247, CuCu−N 1.845, N−O 1.181, ∠CuCuN 177.7, ∠CuNO 136.0	1727.6 (747)
Cu−(NO)−Cu ($^2A'$)	Cu−N 1.889, N−O 1.226, ∠CuNCu 101.3, *D*(CuCuNO) 142[a]	1417.5 (670)
$Cu_2(NO)_2$ (^1A_g)	Cu−N 1.925, N−O 1.216, Cu−Cu 2.834, ∠NCuN 85.2	1492.9 (1403) (b_{1u}) 1552.3 (0) (a_g)

[a] *D* = dihedral angle.

vibrational coupling evidenced in the antisymmetric N−O stretching mode of linear ON−Cu−NO, which is different from that in CuNO.

The reaction of CuNO with another NO molecule proceeds readily on annealing, and exothermic (−36.9 kcal/mol, BP86) reaction 2 is expected from the shorter Cu−N bonds in $Cu(NO)_2$ as compared to CuNO.

$$\mathrm{CuNO}\ (^1\mathrm{A}') + \mathrm{NO}\ (^2\Pi) \rightarrow \mathrm{Cu(NO)_2}\ (^2\Pi) \qquad (2)$$

$Cu(NO)_2(NO)$*. The sharp absorption at 1692.8 cm^{-1} in neon matrix experiments increased markedly on annealing, particularly higher temperature annealing, when $Cu(NO)_2$ increased at the expense of CuNO (Figure 1). This band shifted to 1662.8 cm^{-1} with $^{15}N^{16}O$ and to 1618.9 cm^{-1} with $^{15}N^{18}O$ samples, and gave a $^{14}NO/^{15}NO$ ratio of 1.0180 and a $^{15}N^{16}O/^{15}N^{18}O$ ratio of 1.0271, indicating a N−O stretching vibration. In both mixed $^{14}N^{16}O + {}^{15}N^{16}O$ and $^{15}N^{16}O + {}^{15}N^{18}O$ experiments, sextet band patterns were observed as shown in Figures 2 and 3. These triplet of doublets patterns indicate that the two equivalent NO subunits involved in this vibration are slightly perturbed by another inequivalent NO subunit, and the observed mode is due mainly to the two equivalent NO subunits. This band is assigned to the $Cu(NO)_2(NO)$* complex including two equivalent NO submolecules and another NO with different coordination geometry. The argon matrix counterpart is observed at 1684.9 and 1680.0 cm^{-1}.

The most stable transition metal nitrosyl is $Cr(NO)_4$, and according to the 18-electron rule, $Co(NO)_3$ is expected. This conventional trinitrosyl has been observed in our matrix isolation studies.[32,33] However, copper has two more electrons than cobalt, and the $^2\Pi_u$ state $Cu(NO)_2$ can coordinate one more electron only in a bent nitrosyl configuration.

BP86 calculations find two stable $Cu(NO)_2(NO)$* configurations, and the $^3A''$ state is 8.4 kcal/mol more stable than the $^1A'$ state. Our BP86 frequency calculations predict coincident very strong modes for $Cu(NO)_2(NO)$* ($^3A''$) at 1640 cm^{-1} with 1.0184 ± 0.0002 and 1.0277 ± 0.0002 nitrogen 14/15 and oxygen 16/18 isotopic frequency ratios, in agreement with the observed frequency, which is not the case for the strongest band of the $^1A'$ state. Furthermore, the $^1A'$ state is 1.5 kcal/mol *above* $Cu(NO)_2$ ($^2\Pi_u$) and NO ($^2\Pi_u$), which means that the $^1A'$ state cannot form spontaneously on annealing the matrix. This further supports assignment to the $^3A''$ state $Cu(NO)_2(NO)$* complex, which is formed on annealing in the matrix. The reaction of NO with $Cu(NO)_2$ to form $Cu(NO)_2(NO)$* is exothermic (−6.9 kcal/mol with ZPE correction), which is consistent with growth of $Cu(NO)_2(NO)$* on annealing reaction 3.

$$\mathrm{Cu(NO)_2}\ (^2\Pi_u) + \mathrm{NO}\ (^2\Pi_u) \rightarrow \mathrm{Cu(NO)_2(NO)^*}\ (^3A'') \qquad (3)$$

$CuNO^+$. A weak band at 1907.9 cm^{-1} in the neon matrix experiments increased on annealing and decreased on photolysis, but the isotopic counterparts were overlapped by NO absorption. This band increased relative to that of CuNO with added CCl_4, which suggests a cation species.[21] The 1907.9 cm^{-1} absorption is assigned to the N−O stretching vibration of the $CuNO^+$ cation in solid neon. Both BP86 and B3LYP calculations found a $^2A'$ ground state for $CuNO^+$, in agreement with previous calculations.[13,15] The N−O stretching vibration was predicted at 1878.8 cm^{-1} using BP86 and at 2001.5 cm^{-1} using B3LYP functionals, which are appropriate, with scale factors,[34] for the observed band.

$Cu(NO)_2^-$. The weak band at 1565.2 cm^{-1} on sample deposition in neon slightly decreased on annealing, disappeared on broad-band photolysis, and failed to reproduce on additional higher temperature annealing. This band shifted to 1533.2 cm^{-1} using the $^{15}N^{16}O$ sample and to 1500.8 cm^{-1} using the $^{15}N^{18}O$ sample, and gave a nitrogen 14/15 isotopic ratio of 1.0209 and an oxygen 16/18 isotopic ratio of 1.0216, which are typical N−O stretching vibrational ratios of a nitrosyl species. In both mixed $^{14}N^{16}O + {}^{15}N^{16}O$ and $^{15}N^{16}O + {}^{15}N^{18}O$ experiments, triplets with approximately 1:2:1 relative intensities were observed with intermediates at 1544.3 and 1511.3 cm^{-1}, indicating that two equivalent NO submolecules are involved in this vibration. The 1565.2 cm^{-1} band was eliminated by doping with CCl_4 to trap electrons from the ablation process, which strongly suggests the anion assignment.[21−23] This band is assigned to the antisymmetric N−O stretching vibration of the $Cu(NO)_2^-$ anion. The argon matrix counterpart was observed at 1551.2 cm^{-1}, which exhibited the same annealing, photolysis, and CCl_4 doping behavior and had the same isotopic frequency ratios. The 14 cm^{-1} argon-to-neon matrix shift is common for anion species recently identified.[21−23]

The $Cu(NO)_2^-$ anion assignment is further confirmed by DFT calculations. At the BP86/6-311+G(d) level of theory, $Cu(NO)_2^-$ was predicted to have a linear $^1\Sigma_g^+$ ground state, with a bent $^3B_2$ state lying 9.4 kcal/mol higher in energy. The antisymmetric N−O stretching vibration is calculated at 1577.5 cm^{-1}, which is in good agreement with the observed value. The antisymmetric ON−Cu−NO stretching mode was calculated at 661.6 cm^{-1} with much lower intensity, and is not observed here. Again, the B3LYP calculation predicted the relative stability of the $^1\Sigma_g^+$ and $^3B_2$ states incorrectly. Finally, there is no evidence for $CuNO^-$ anion in both argon and neon matrix experiments. The $CuNO^-$ anion was predicted to have a $^2A''$ ground state, with an N−O stretching vibrational frequency at 1399.7 cm^{-1} (BP86) and 1454.8 cm^{-1} (B3LYP), and is probably too weak to be observed here.

$Cu_2(NO)_x$. A 1499.6 cm^{-1} band in neon experiments increased on higher temperature annealing, shifted to 1473.7 and 1433.8 cm^{-1} using $^{15}N^{16}O$ and $^{15}N^{18}O$ samples, and gave an isotopic 14/15 ratio of 1.0176 and a 16/18 ratio of 1.0278, indicating a N−O stretching vibration. This region is too low for terminal N−O stretching vibrations, so bridge-bonded species should be considered. In both mixed $^{14}N^{16}O + {}^{15}N^{16}O$ and $^{15}N^{16}O + {}^{15}N^{18}O$ experiments, triplets with approximately 1:2:1 relative intensities were observed; accordingly this band is considered for the bridge-bonded $Cu_2(NO)_2$ molecule. DFT calculation predicted a ^1A_g ground-state $Cu_2(NO)_2$ with a strong b_{1u} mode at 1492.9 cm^{-1}, which is in excellent agreement with

the observed value, and indicates the $Cu_2(NO)_2$ assignment. There is no obvious band in argon matrix experiments that can be assigned to the $Cu_2(NO)_2$ molecule; it appears that Cu atoms diffuse more easily in neon and form the stable $Cu_2(NO)_2$ molecule.

Additional weak bands at 1734.8 and 1515.9 cm^{-1} appeared only in argon matrix experiments, where higher laser power was employed. These two bands increased on annealing, and only pure isotopic counterparts were present in the mixed $^{14}N^{16}O + {}^{15}N^{18}O$ experiments, indicating one NO involvement in these vibrational modes. The 1734.8 cm^{-1} band is in the terminal N−O stretching vibrational frequency region, while the 1515.9 cm^{-1} band is in the frequency region expected for bridged species, so a Cu_2NO species is the first to be considered. Previous quantum chemical studies of NO interacting with Cu_2 found that bonding occurs preferably at the linear end-on CuCuNO geometry rather than the bridge-bonded Cu−(NO)−Cu geometry.[20] Our DFT calculation obtained similar results, as listed in Table 6. The $^2A'$ state end-on CuCuNO is 15.9 kcal/mol lower in energy than the $^2A'$ state bridge-bonded Cu−(NO)−Cu species, and the N−O stretching vibrations for end-on and bridge-bonded Cu_2NO are 1787.3 and 1417.5 cm^{-1}. The 1734.8 cm^{-1} band fits the 1787.3 cm^{-1} calculated frequency for the end-on Cu_2NO molecule quite well, so this assignment can be proposed from the DFT calculation. However, the 1515.9 cm^{-1} band does not fit the 1417.5 cm^{-1} value calculated for bridge-bonded Cu_2NO, so this molecule cannot be identified. Another possibility is the CuON isomer. Previous calculations found that CuON is also a stable molecule but slightly higher (about 7 kcal/mol) in energy than the CuNO isomer.[13] As listed in Tables 3 and 4, both BP86 and B3LYP functionals predict that CuON is slightly higher in energy than CuNO. The N−O stretching frequency of CuON is calculated as 1400.4 cm^{-1} (B3LYP) and 1430.1 cm^{-1} (BP86), which do not agree with the observed 1515.9 cm^{-1} band, so CuON cannot be assigned.

$CuNO_2$. A weak absorption at 1214.5 cm^{-1} in neon experiments appeared only on higher temperature annealing; this band shifted to 1191.4 cm^{-1} using the $^{15}N^{16}O$ sample and to 1163.4 cm^{-1} using the $^{15}N^{18}O$ sample. In the mixed $^{14}N^{16}O + {}^{15}N^{16}O$ experiment, only pure isotopic counterparts were presented, while in the mixed $^{15}N^{16}O + {}^{15}N^{18}O$ spectra, a triplet with an intermediate at 1174.9 cm^{-1} was observed, indicating that only one N and two equivalent O atoms are involved in this mode. This band is assigned to the antisymmetric ONO stretching vibration of the bidentate Cu−(η^2-O,O)N molecule, which is formed by reactions of Cu atoms with NO_2 molecules. The 1213.4 cm^{-1} band in argon matrix experiments showed the same behavior, and is due to the Cu−(η^2-O,O)N molecule in argon. Sodupe and co-workers[35] have calculated the structure, binding energy, and vibrational frequencies for $CuNO_2$ in different coordination modes; the C_{2v} bidentate Cu−(η^2-O,O)N coordination was predicted to be the most stable structure. Our BP86/6-311+G(d) calculation predicted a $^1A_1$ ground-state Cu−(η^2-O,O)N molecule with Cu−O and N−O bond lengths of 2.119 and 1.263 Å, and ∠ONO = 115°; the antisymmetric N−O stretching vibration is calculated at 1260.5 cm^{-1}, which is in good agreement with observed values. Worden and Ball[36] assigned a 1220 cm^{-1} band in argon to $Cu^+NO_2^-$, and a 1214 cm^{-1} band to the $Cu(NO_2)_2$ molecule. It appears that their 1214 cm^{-1} band corresponds to our 1213.4 cm^{-1} band in argon, and should be assigned to the Cu−(η^2-O,O)N molecule instead of $Cu(NO_2)_2$.

OCuNO. The weak band at 1852.2 cm^{-1} in the argon matrix increased on annealing, markedly decreased on photolysis, and partly reproduced on further annealing (Figure 5). The $^{15}N^{16}O$ counterpart was observed at 1816.2 cm^{-1}, which gave a $^{14}NO/{}^{15}NO$ ratio of 1.0198. In the mixed $^{14}N^{16}O + {}^{15}N^{16}O$ experiments, only pure isotopic counterparts were present. The argon matrix experiments employed higher laser energy and also observed the $^{63}CuO/{}^{65}CuO$ doublet at 627.7 and 625.8 cm^{-1}.[37] As expected from the Co and Ni experiments, the 1852.2 cm^{-1} band is assigned to the OCuNO complex. The much weaker interaction between CuO and NO is indicated by the 20 cm^{-1} red shift in the NO fundamental as compared to CuNO, which sustains a 285 cm^{-1} red shift. Our BP86 calculation predicts 1890.0 cm^{-1} for the N−O fundamental in the OCuNO complex, near the 1883.9 cm^{-1} value calculated for NO itself.

Comparisons with Cu−Nitrosyl Species in Zeolites. The nitrosyl frequencies of $CuNO^+$ (1907.9 cm^{-1}) and CuNO (1602.2 cm^{-1}) show a pronounced dependence on net charge. The calculated Mulliken charges show that most of the net charge resides on the metal (Table 3). Adding one electron decreases the Cu−N bond length and increases the N−O bond length, thus decreasing the N−O stretching vibrational frequency. Hence, the nitrosyl stretching frequency provides a rough measure of charge on the CuNO species, which approximates local charge on the CuNO center.

It is generally accepted that Cu-exchanged zeolites contain a mixture of Cu^+ and Cu^{2+} ions, coordinated to the zeolite lattice and charge compensated by anionic Al T-sites, and possibly by extra lattice ions in the Cu^{2+} case.[2] Both Cu^+ and Cu^{2+} sites are observed to adsorb single NO molecules. The N−O stretching frequency for Cu(I)−NO/zeolite is reported near 1800 cm^{-1} depending on the zeolite,[2,5] which is about 2/3 of the way between our CuNO and $CuNO^+$ frequencies, and a +0.7 net charge on the CuNO center is proposed. An average Cu(II)−NO/zeolite frequency[5] at 1900 cm^{-1} is near our $CuNO^+$ frequency, which suggests a +1.0 net charge on the CuNO center for this *formally* Cu(II) NO/zeolite species.

Copper cation sites in zeolite can also adsorb two NO molecules to form Cu−*gem*-dinitrosyl species, which have been suggested to play an important role in NO decomposition.[2,5,7] This dinitrosyl species is bent, with comparable intensities for symmetric and antisymmetric N−O vibrations observed at 1824 and 1727−1738 cm^{-1} in Cu−ZSM.[5] The $Cu(NO)_2$ species observed in our experiments is linear. However, our DFT calculations predict that both bent $Cu(NO)_2^+$ and $Cu(NO)_2$ are stable. The symmetric and antisymmetric N−O stretching vibrations of the bent $^1A_1$ state $Cu(NO)_2^+$ are 2−4% lower than for the linear $^3\Sigma_g^-$ state $Cu(NO)_2^+$, and the $^2B_1$ state $Cu(NO)_2$ frequencies are 6−9% lower than for the $^2\Pi_u$ state $Cu(NO)_2$. If the calculated frequencies for bent $Cu(NO)_2$ and $Cu(NO)_2^+$ are scaled by a factor of 0.94 from those of our observed linear dinitrosyl species, the Cu−*gem*-dinitrosyl frequencies are approximately equal to the scaled 1789 and 1731 cm^{-1} values for bent $Cu(NO)_2^+$. Therefore, we conclude that the net charge on Cu−*gem*-dinitrosyl is approximately +1. Charges have been estimated for Rh(I)CO and Rh(I)$(CO)_2$ on zeolites from RhCO and $Rh(CO)_2$ spectra in solid neon and DFT calculations.[23]

Conclusions

In summary, laser-ablated copper atoms react with NO molecules in excess neon and argon during condensation to form the CuNO and $Cu(NO)_2$ molecules as major products. In addition, the $CuNO^+$ cation and $Cu(NO)_2^-$ anion are also formed. These copper nitrosyl species were identified from isotopic shifts and mixed isotopic patterns in the matrix infrared spectra and supported by DFT calculations of isotopic frequen-

cies. Isotopic spectra are also presented for $Cu(NO)_2(NO)$* with different (NO)* coordination, which follows the 18-electron rule. Evidence is found for a bridge-bonded $Cu_2(NO)_2$ species and a copper oxide complex, OCuNO. Finally, the isolated mononitrosyl species provide a scale to estimate local charge on CuNO sites in Cu-exchanged zeolite catalyst systems.

Acknowledgment. We gratefully acknowledge NSF support for this research under Grant CHE 97-00116.

References and Notes

(1) Iwamoto, M.; Furukawa, H.; Mine, Y.; Uemera, F.; Mikuriya, S.; Kagawa, S. *J. Chem. Soc., Chem. Commun.* **1986**, 1272.

(2) Shelef, M. *Chem. Rev.* **1995**, *95*, 209.

(3) Spoto, G.; Bordiga, S.; Scarano, D.; Zecchina, A. *Catal. Lett.* **1992**, *13*, 39. Spoto, G.; Zecchina, A.; Bordiga, S.; Richiardi, G.; Mata, G. *Appl. Catal., B* **1994**, *3*, 151.

(4) Iwamoto, M.; Yahiro, H.; Mizuno, N.; Zhang, X. W., Mine, Y.; Furukawa, H.; Kagawa, S. *J. Phys. Chem.* **1992**, *96*, 8360. Iwamoto, M.; Yokoo, S.; Saki, K.; Kagawa, S. *J. Chem. Soc., Faraday Trans. 1* **1981**, *77*, 1629.

(5) Valyon, J.; Hall, W. K. *J. Phys. Chem.* **1993**, *97*, 1204.

(6) Aylor, A. W.; Larsen, S. C.; Reimer, J. A.; Bell, A. T. *J. Catal.* **1995**, *157*, 592.

(7) Beutel, T.; Sarkany, J.; Lei, G. D.; Yan, J. Y.; Sachtler, W. M. H. *J. Phys. Chem.* **1996**, *100*, 845.

(8) Cheung, T.; Bhargava, S. K.; Hobday, M.; Foger, K. *J. Catal.* **1996**, *158*, 301.

(9) Schneider, W. F.; Ramprasad, R.; Hass, K. C.; Adams, J. B. *J. Phys. Chem.* **1996**, *100*, 6030.

(10) Ramprasad, R.; Hass, K. C.; Schneider, W. F.; Adams, J. B. *J. Phys. Chem. B* **1997**, *101*, 6903.

(11) Sulzle, D.; Schwarz, H.; Moock, K. H.; Terlouw, J. K. *Int. J. Mass Spectrom. Ion Processes* **1991**, *108*, 269.

(12) Chiarelli, J. A.; Ball, D. W. *J. Phys. Chem.* **1994**, *98*, 12828. see also: Ruschel, G. K.; Nemetz, T. M.; Ball, D. W. *J. Mol. Struct.* **1996**, *384*, 101.

(13) Hrusak, J.; Koch, W.; Schwarz, H. *J. Chem. Phys.* **1994**, *101*, 3898.

(14) Benjelloun, A. T.; Daoudi, A.; Berthier, G.; Rolando, C. *THEOCHEM* **1996**, *360*, 127.

(15) Thomas, J. L. C.; Bauschlicher, C. W., Jr.; Hall, M. B. *J. Phys. Chem. A* **1997**, *101*, 8530.

(16) Blanchet, C.; Duarte, H. A.; Salahub, D. R. *J. Chem. Phys.* **1997**, *106*, 8778.

(17) So, S. K.; Franchy, R.; Ho, W. *J. Chem. Phys.* **1991**, *95*, 1385.

(18) Kinoshita, I.; Misu, A.; Munchata, T. *J. Chem. Phys.* **1994**, *102*, 2970.

(19) Illas, F.; Ricart, J. M.; Fernandez-Garcia, M. *J. Chem. Phys.* **1996**, *104*, 5647.

(20) Rochefort, A.; Fournier, R. *J. Phys. Chem.* **1996**, *100*, 13506.

(21) Zhou, M. F.; Andrews, L. *J. Chem. Phys.* **1999**, *110*, 10370.

(22) Zhou, M. F.; Andrews, L. *J. Am. Chem. Soc.* **1998**, *120*, 11499.

(23) Zhou, M. F.; Andrews, L. *J. Am. Chem. Soc.* **1999**, *121*, 9171.

(24) Burkholder, T. R.; Andrews, L. *J. Chem. Phys.* **1991**, *95*, 8697.

(25) Andrews, L.; Zhou, M. F.; Willson, S. P.; Kushto, G. P.; Snis, A.; Panas, I. *J. Chem. Phys.* **1998**, *109*, 177.

(26) Andrews, L.; Zhou, M. F. *J. Chem. Phys.* **1999**, *111*, 6036.

(27) Frisch, M. J.; Trucks, G. W.; Schlegel, H. B.; Gill, P. M. W.; Johnson, B. G.; Robb, M. A.; Cheeseman, J. R.; Keith, T.; Petersson, G. A.; Montgomery, J. A.; Raghavachari, K.; Al-Laham, M. A.; Zakrzewski, V. G.; Ortiz, J. V.; Foresman, J. B.; Cioslowski, J.; Stefanov, B. B.; Nanayakkara, A.; Challacombe, M.; Peng, C. Y.; Ayala, P. Y.; Chen, W.; Wong, M. W.; Andres, J. L.; Replogle, E. S.; Gomperts, R.; Martin, R. L.; Fox, D. J.; Binkley, J. S.; Defrees, D. J.; Baker, J.; Stewart, J. P.; Head-Gordon, M.; Gonzalez, C.; Pople, J. A. *Gaussian 94*, Revision B.1; Gaussian, Inc.: Pittsburgh, PA, 1995.

(28) Perdew, J. P. *Phys. Rev. B* **1986**, *33*, 8822. Becke, A. D. *J. Chem. Phys.* **1993**, *98*, 5648.

(29) Lee, C.; Yang, E.; Parr, R. G. *Phys. Rev. B* **1988**, *37*, 785.

(30) McLean, A. D.; Chandler, G. S. *J. Chem. Phys.* **1980**, *72*, 5639. Krishnan, R.; Binkley, J.S.; Seeger, R.; Pople, J. A. *J. Chem. Phys.* **1980**, *72*, 650.

(31) Wachters, H. J. H. *J. Chem. Phys.* **1970**, *52*, 1033. Hay, P. J. *J. Chem. Phys.* **1977**, *66*, 4377.

(32) Zhou, M. F.; Andrews, L. *J. Phys. Chem. A* **1998**, *102*, 7452 (Cr + NO).

(33) Zhou, M. F.; Andrews, L. *J. Phys. Chem. A* **2000**, in press. (Fe, Co, Ni + NO).

(34) Bytheway, I.; Wong, M. W. *Chem. Phys. Lett.* **1998**, *282*, 219.

(35) Rodriguez-Santiago, L.; Branchadell, V.; Sodupe, M. *J. Chem. Phys.* **1995**, *103*, 9738.

(36) Worden, D.; Ball, D. W. *J. Phys. Chem.* **1992**, *96*, 7167.

(37) Chertihin, G. V.; Andrews, L.; Bauschlicher, C. W., Jr. *J. Phys. Chem. A* **1997**, *101*, 4026 (Cu + O_2).